Environmental Science and Pollution Research (2021) 28:57619–57628
https://doi.org/10.1007/s11356-021-14649-0

RESEARCH ARTICLE

Application of plasma catalysis system for C_4F_8 removal

Ya Sheng Chen[1] · Kuan Lun Pan[1,2] · Moo Been Chang[1]

Received: 7 March 2021 / Accepted: 26 May 2021 / Published online: 5 June 2021

Abstract

Octafluorocyclobutane (C_4F_8) with a GWP_{100} (global warming potential) of 10,000 times of CO_2 is listed as potent greenhouse gas. Therefore, development of effective control technologies for reducing C_4F_8 emissions has become an emerging issue to be addressed. In this study, decomposition of C_4F_8 was investigated via three systems including catalytic hydrolysis, non-thermal plasma, and plasma catalysis, respectively. Decomposition of C_4F_8 achieved with catalytic hydrolysis reaches the highest efficiency of 20.1%, being obtained with γ-Al_2O_3 as catalyst in the presence of 10% $H_2O_{(g)}$ and operating temperature of 800 °C. For plasma-based system, the highest C_4F_8 conversion obtained with non-thermal plasma is 62% at a voltage of 23 kV. As for the plasma catalysis system, 100% C_4F_8 conversion efficiency can be achieved at an applied voltage of 22–23 kV. The effects of various parameters such as gas flow rate and C_4F_8 concentration on plasma-based system show that the plasma catalysis also has better resistivity for the high gas flow rate. The highest energy efficiency of 0.75 g/kWh is obtained for the gas flow rate of 500 mL/min, with the C_4F_8 conversion of 41%. The highest conversion 89% was achieved with the O_2 content of 0.5%. Addition of Ar improves the performance of plasma-based system. When Ar is controlled at 20%, C_4F_8 conversions obtained with plasma catalysis reach 100% at applied voltage of 22–23 kV even in the presence of 5% O_2. The main products of the C_4F_8 conversion include CO_2, NO_x, and COF_2 when O_2 is added into the system. As water vapor is added, HF is also formed. This study has confirmed that combined non-thermal plasma with catalyst system to convert C_4F_8 is indeed feasible and has good potential for further development.

Keywords Octafluorocyclobutane (C_4F_8) · γ-Al_2O_3 · Non-thermal plasma · Plasma catalysis

Introduction

Perfluorocarbons (PFCs) are widely used in the semiconductor industry despite their nature as an extremely potent greenhouse gas that contributes to global warming (Kuroki et al. 2005). PFCs are composed of carbon, sulfur, or nitrogen as the central atom bonded with the fluorine atoms such as in CF_4, C_2F_6, C_3F_8, C_4F_8, SF_6, and NF_3 (Lin et al. 2011; Chang and Yu 2001). According to the Taiwan Semiconductor Industry Association (TSIA), the annual usage of PFCs in Taiwan's semiconductor industry is over 300 metric tons. These PFCs are mostly inert and non-corrosive gases that intensely absorb infrared radiation. Consequently, PFCs are capable of affecting the greenhouse effect of the earth. C_4F_8 has an atmospheric lifetime of 3200 years (16 times higher than CO_2) and GWP_{100} (global warming potential) of 10,000 (Suzuki et al. 2008). Thus, effective reduction of C_4F_8 emission has become an emerging issue.

Optimized process with alternative chemicals is commonly applied to reduce the amount of PFCs used in the industry. However, destruction of PFCs via combustion (Jia and Ma 2005), catalytic reduction, and plasma abatement (Lee and Chen 2017) is generally considered as the most effective PFCs reduction strategy. The removal efficiency of PFCs achieved with combustion reaches ≥ 99%, but it has high-energy consumption (Chang and Chang 2006). On the other hand, catalytic hydrolysis is one of the most practical and economical methods for reducing PFCs (Lee and Jeon 2012; Park et al. 2012). Takita et al. (1999) described the decomposition of PFCs via hydrolysis with selected metal phosphate catalysts such as aluminum phosphate ($AlPO_4$). However, the system needs to be operated at high temperatures (≥ 600 °C).

Responsible Editor: Santiago V. Luis

✉ Moo Been Chang
mbchang@ncuen.ncu.edu.tw

[1] Graduate Institute of Environmental Engineering, National Central University, No.300, Zhongda Road, Zhongli District, Taoyuan City 32001, Taiwan

[2] Green Energy and Environmental Institute, Industrial Technology Research Institute, Hsinchu, Taiwan

Various Al_2O_3-based catalysts have been investigated for the conversion CF_4 through catalytic hydrolysis. For instance, Song et al. (2013) used Ce/Al_2O_3 as a catalyst for the hydrolysis of CF_4. The results show that the highest removal of CF_4 reached with Ce/Al_2O_3 is 63%. Relevant study denotes that alumina-based bimetallic oxides such as $Ga\text{-}Al_2O_3$ or $Ni\text{-}Al_2O_3$ could promote the catalytic hydrolysis of CF_4 (Takita et al. 2002) . According to Pan et al. (2019) $\gamma\text{-}Al_2O_3$ could achieve 72% CF_4 conversion at 900 °C, through thermal catalysis. However, the catalyst system needs a high operating temperature (≥ 800 °C) to obtain good performance. Besides, the catalysts are susceptible to poisoning by fluorine, sulfur, and particulate matter (Zhang et al. 2018a).

Non-thermal plasma (NTP) has been demonstrated effective in removing PFCs (Gao et al. 2011). It has the advantages of rapid startup, high operating flexibility, and low equipment cost, but it has the disadvantage of low-energy efficiency (Futamura et al. 2001). Recently, combining non-thermal plasma with catalyst has been investigated as one of viable technologies towards PFC destruction (Futamura and Gurusamy 2005). This technology improves the shortcomings of the plasma system and induces synergistic effects with the catalyst (Chen et al. 2008). So far, plasma catalysis technology has been applied for VOCs removal and hydrocarbon reforming to produce hydrogen (Chen et al. 2008; Kim et al. 2008; Chen et al. 2017). However, relevant studies on PFCs removal are limited. Compared with non-thermal plasma system, plasma catalysis system has the following advantages: high contaminant/reactant conversion efficiency, improved selectivity for harmless by-products, and improved energy efficiency (Chang and Lee 2004).

In this study, removal of C_4F_8 from gas streams through catalytic hydrolysis is first evaluated with $\gamma\text{-}Al_2O_3$ as catalyst. As mentioned previously, $\gamma\text{-}Al_2O_3$ shows good capability to decompose PFC because its Lewis acid site could break down the strong C-F bond, while the production cost is reasonable and suitable for industrial application. In brief, the plasma-based system used in this study includes non-thermal plasma and plasma catalysis system.

Experimental

Plasma system

The performance of $\gamma\text{-}Al_2O_3$ for the removal of C_4F_8 via catalytic hydrolysis is firstly evaluated. A quartz tube with an inner diameter of 20 mm and the length of 300 mm is employed as reactor. Inlet gas consists of 300 ppm C_4F_8, 0–10% of $H_2O_{(g)}$, and N_2 as balance gas. C_4F_8 and N_2 were provided by gas cylinders, while $H_2O_{(l)}$ was introduced into the system by a peristaltic pump and evaporated to form $H_2O_{(g)}$. The gas flow rate was regulated by mass flow controllers (MFCs) to 100 mL/min, and the gas hourly space velocity (GHSV) was controlled at 6000 h^{-1}, and the system was operated at a temperature ranging from 300 to 800°C.

The schematic diagram of the experimental system for the removal of C_4F_8 via plasma-based systems is shown in Fig. 1. The plasma-based system with a dielectric barrier discharge (DBD)-type reactor was applied to a series of tests. DBD reactor was mainly a quartz tube with the inner diameter of 20 mm and length of 300 mm. The grounded electrode is aluminum foil with length = 94 mm wrapped outside, and stainless-steel rod with outside diameter = 3 mm was used as inner electrode. The total discharge volume was fixed at 27.6 cm^3. All plasma-based experiments including non-thermal plasma and plasma catalysis were operated with the inlet C_4F_8 concentration of 300 ppm, and N_2 as carrier gas was imported into the plasma-based systems for reaction. Furthermore, the effects of gas flow rate ranging from 100 to 1,500 mL/min, C_4F_8 concentration ranging from 300 to 10,000 ppm, and addition of O_2 and Ar are evaluated. N_2, Ar, and O_2 were provided by gas cylinders. An AC power with medium frequency (You-Shang, Taiwan) was used as the power supply, and the highest applied voltage and frequency are 23 kV and 18.5 kHz, respectively. The power consumption was measured via a digital oscilloscope (Tektronix DPO3014, USA) equipped with a current probe (Tektronix TCPA300, USA) and a high-voltage probe (Tektronix P6015A, USA). All by-products were monitored by a Fourier transform infrared spectrophotometer (FTIR, Nicolet 6700, USA Thermo Scientific, USA). All experimental data would be recorded as the reaction reached steady state. For the analysis of the experimental results, conversion efficiency (η) of C_4F_8 and energy efficiency are shown by Eqs. (1)–(2), respectively:

$$\eta\ (\%) = \frac{[C_4F_8]_{in} - [C_4F_8]_{out}}{[C_4F_8]_{in}} \times 100\% \quad (1)$$

$$\text{Energy efficiency (g/kWh)} = \frac{\text{Mass flow rate}\left(\frac{g}{h}\right) \times \eta}{P(kW)} \quad (2)$$

Catalyst characterization

Commercial $\gamma\text{-}Al_2O_3$ applied as catalyst was characterized by transmission electron microscope (TEM), Brunauer-Emmett-Teller (BET) surface areas, and X-ray diffraction (XRD). Transmission electron microscope (JEM2000FX JEOL, Japan) is applied to observe the morphology of catalyst (Fig. S1). ASAP2010 (Micromeritics, USA) was applied for the measurement of the BET surface area (S_{BET}) via the adsorption-desorption process with N_2 at − 196 °C. X-ray

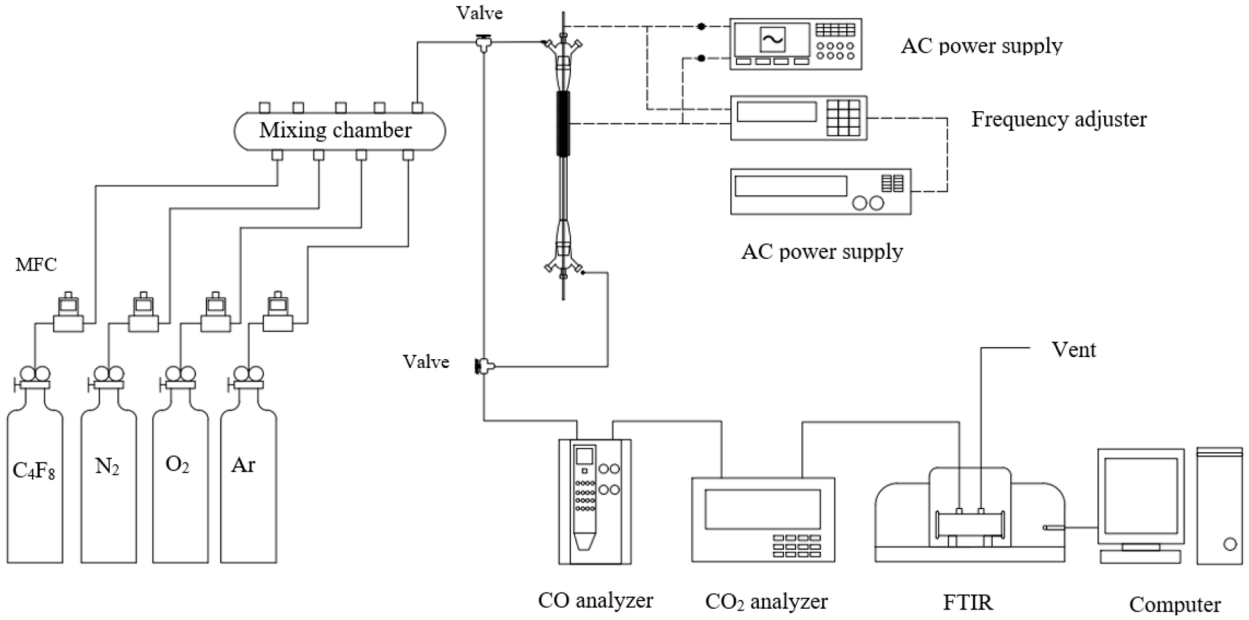

Fig. 1 Plasma-based systems for C_4F_8 removal

diffraction (XRD) was performed with X-ray diffractometer (D8AXRD BRUKER, Germany) at 40 kV and 10 mA by using Cu-Kα radiation, and XRD profiles were obtained at a 2θ range of 10–80° with a scanning rate of 6°/min (see Fig. S2). The results of catalyst characterization are presented in Supporting Information (Table S1).

Results and discussion

Catalytic hydrolysis of C_4F_8 removal

Figure 2 shows the C_4F_8 conversions obtained with catalytic hydrolysis operated at different temperatures, with γ-Al_2O_3 as catalyst for the following conditions: [C_4F_8] = 300 ppm, [$H_2O_{(g)}$] = 0–10%, [GHSV] = 6000 h^{-1}. When the operating temperature is ≤ 500 °C, the C_4F_8 removal efficiency is 0% for the gas stream containing 0–10% $H_2O_{(g)}$. C_4F_8 conversion increases slightly with increasing temperature, and the highest removal efficiency reaches 5.2% in the absence of $H_2O_{(g)}$ at 800 °C. The C_4F_8 conversion efficiency obtained with γ-Al_2O_3 reaches 11.3% in the presence of 5% $H_2O_{(g)}$ when it is operated at 600 °C. As $H_2O_{(g)}$ content is increased to 10%, C_4F_8 removal efficiency further increases to 20.1% with the operating temperature of 800 °C. Conversion of C_4F_8 increases with increasing $H_2O_{(g)}$ content, implying that increasing $H_2O_{(g)}$ content facilitates catalytic hydrolysis of C_4F_8. Mechanisms of C_4F_8 hydrolysis with γ-Al_2O_3 as catalyst are illustrated in Fig. 3 (Kuroki et al. 2005). The first step of catalytic hydrolysis of C_4F_8 is the adsorption of C_4F_8 molecules on the active sites of γ-Al_2O_3. Subsequently, the O atom on metal oxide containing Lewis acid breaks the C-F bond on C_4F_8 to form M-O-C_xF_y and M-C_xF_y. M-O-C_xF_y is then hydrolyzed to form M-OH and CHF_2, while M-C_xF_y is further hydrolyzed to form M-OH, C_xF_y-OH, HF, and CO_2. Eventually, M-OH that reacted with another M-OH was regenerated to form γ-Al_2O_3. $H_2O_{(g)}$ was released simultaneously as a by-product. On the other hand, C_xF_y-OH was hydrolyzed until termination. The M (in M-OH) indicates metals, and L (in L-acid) indicates Lewis acid. Under similar operating condition, El-Bahy et al. (2003) apply γ-Al_2O_3 to decompose CF_4, and the main product is CO_2.

The acidic site on surface of catalyst plays a significant role in conversion of fluorocarbon (Jie et al. 2008). The results

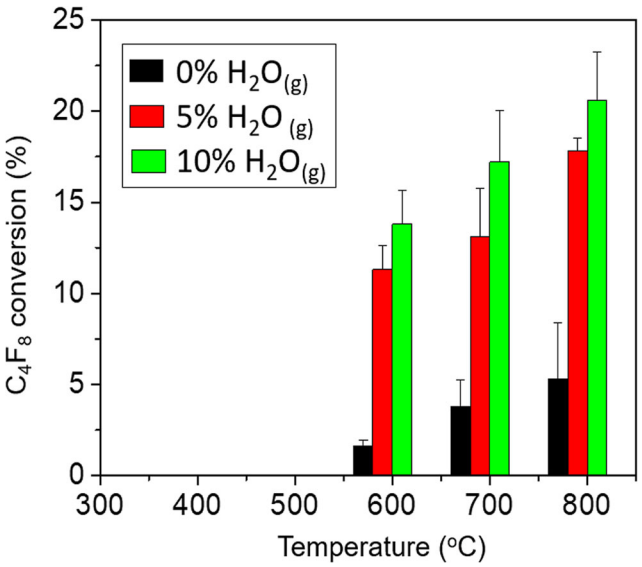

Fig. 2 C_4F_8 conversion achieved with catalytic hydrolysis at various operating temperatures ([C_4F_8] = 300 ppm, [$H_2O_{(g)}$] = 0–10%, carrier gas = N_2, [GHSV] = 6000 h^{-1})

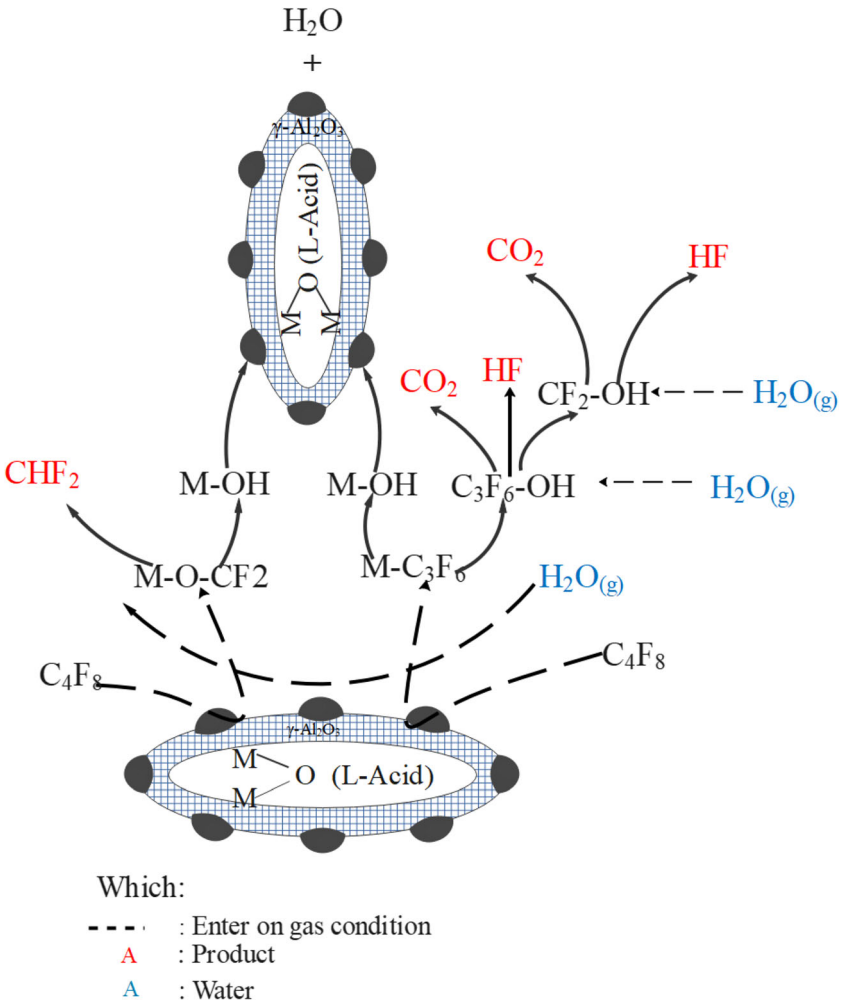

Fig. 3 Mechanisms of catalytic hydrolysis of C_4F_8 with γ-Al_2O_3 as catalyst

obtained in this study indicate that only moderate C_4F_8 removal could be obtained by hydrolysis with γ-Al_2O_3 as a catalyst when operated at a temperature ranging from 600 to 800 °C. However, high PFCs conversion efficiency is difficult to achieve under mild operating conditions because of high C-F bonding energy (543 ± 4 kJ/mol) and chemical stability (Hannus 1999). Song et al. (2013) show that deactivation of catalyst in the decomposition of fluorocarbon is induced by the formation of HF and the transformation of γ-Al_2O_3 into AlF_3. Moreover, high operating temperature also triggers the deactivation of the catalyst. It is interesting to note that 100% PFCs conversion can be achieved when operated at 900 °C even though the phase transformation from γ-Al_2O_3 into α-Al_2O_3 is inevitable (Jia et al. 2011).

Performances of plasma-based systems for C_4F_8 conversion

Performances of plasma-based systems including non-thermal plasma and plasma catalysis are investigated individually for C_4F_8 conversion with the applied voltage ranging from 12 to 23 kV. As shown in Fig. 4, non-thermal plasma system shows the trend of increasing C_4F_8 conversion by increasing applied voltage. As the applied voltage is increased, higher electron

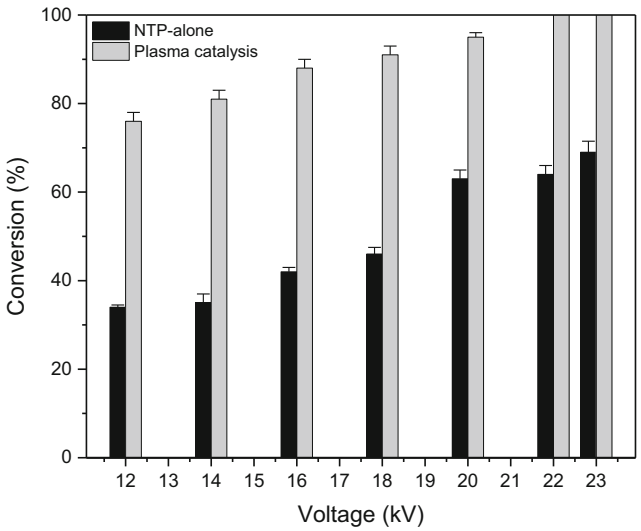

Fig. 4 Performances of plasma-based systems at various applied voltages for C_4F_8 conversion ($[C_4F_8]$ = 300 ppm, carrier gas = N_2, gas flow rate = 100 mL/min)

field is produced, which in turn increases the number of energetic electrons. Hence, the highest C_4F_8 conversion of non-thermal plasma system is achieved at the highest applied voltage. The C_4F_8 conversion of 62% can be reached with the applied voltage of 23 kV. In contrast with the non-thermal plasma system, 100% C_4F_8 conversion is obtained with plasma catalysis when operated with the applied voltage ranging from 22 to 23 kV. These results show that plasma catalysis system has excellent performance for C_4F_8 conversion and the performance of C_4F_8 conversion could be greatly improved as γ-Al_2O_3 is placed into the discharge zone. The combination of the γ-Al_2O_3 catalyst with plasma can increase the conversion value of C_4F_8 in terms of both plasma chemistry and the performance of the plasma. Plasma chemistry condition from γ-Al_2O_3 should occur when the applied voltage was increased. When the applied voltage was increased, more energetic electrons were produced. Eventually, the magnitude of mean electric field should increase too. Inside the plasma system, the collision of energetic electron with C_4F_8 is considered as the most important mechanism leading to C_4F_8 conversion. The possible reaction pathways of energetic electron between C_4F_8 with non-thermal plasma system are given in Fig. 5a. $N_2(A^3\sum_u^+)$ has the characteristic as active species to decompose C_4F_8 with excitation energy of 6.17 eV (Takita et al. 2002). Hence, it is important to note that $N_2(A^3\sum_u^+)$ plays a crucial role in C_4F_8 conversion. Addition of O_2 into non-thermal plasma produces O radicals, resulting in the collision with C_xF_y radicals to form CO, CO_2, COF_2, FO, FO_2, and FNO_2.

Plasma catalysis chemistry is very complicated; it consists of electrons, ions, and exciting species. Possible reactions of energetic electrons with C_4F_8 via plasma catalysis are given in Fig. 5b. The first step of plasma catalysis is the reaction of C_4F_8 with the electron in plasma to form C_xF_y radicals including C_3F_7, C_3F_6, C_3F_5, CF_3, CF_2, and CF. C_4F_8 and C_xF_y radicals were adsorbed on the active sites of γ-Al_2O_3 catalysts. Subsequently, intermediates (M-O-C_xF_y) were formed as O atoms on the catalysts attack and break the C-F bond of the adsorbed C_4F_8. The O atom of other metal oxide or O radical (from addition O_2) attacks the C-F bond of M-O-C_xF_y to form CO, CO_2, and C_xF_y. M-O-C_xF_y continued to lose its C atom until M-O-F_y is formed. Addition of O_2 into plasma-based system produces O radical and leads to the collision with CF_3 and CF to form CO, CO_2, and COF_2 (Hayashi and Satoh 2005; Vasenkov et al. 2004). Besides, N_2* and $N_2(A^3\sum_u^+)$ generated by non-thermal plasma are active to convert C_4F_8. As explained in reactions (3)~(5), $N_2(A^3\sum_u^+)$ plays a crucial role in non-thermal plasma to the removal of gaseous pollutants if N_2 is applied as the carrier gas (Radoiu 2004; Choi et al. 2012).

$$e + N_2 \rightarrow e + N_2^* \quad (3)$$

$$e + N_2 \rightarrow e + N_2\left(A^3\sum_u^+\right) \quad (4)$$

$$N_2^* \text{ or } N_2\left(A^3\sum_u^+\right) + C_4F_8 \rightarrow \text{products} \quad (5)$$

Integration of plasma with catalyst results in the generation of micro-discharge and increased mean electric field due to the contact point between catalysts. One important parameter that affects C_4F_8 conversion and performance of the plasma is dielectric constant of the catalyst that is placed in the discharge zone. In this study, the dielectric constant of γ-Al_2O_3 applied is 9.1.

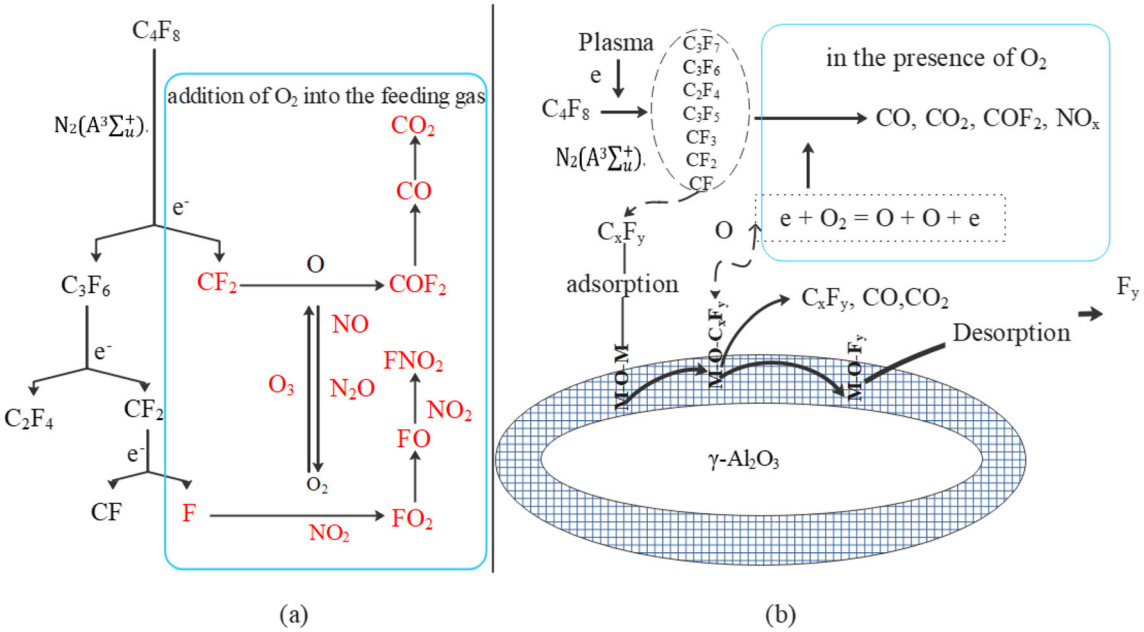

Fig. 5 Possible reactions pathways for C_4F_8 conversion achieved with (**a**) non-thermal plasma and (**b**) plasma catalysis, respectively

Previous studies confirmed that the value of dielectric constant greatly affects plasma performance as shown in the Eqs. (6)–(8) (Takaki et al. 2004; Zhang et al. 2016). According to the equations, the dielectric constant (ε_p) can increase the value of the average electrical field (E_x), electron density (n_e), and mean electron energy (E_e) which can result in the increase of energy distribution function (EEDF) and electron temperature.

$$E_x \approx \frac{V}{d}\frac{3\varepsilon_p}{2\varepsilon_p + \varepsilon_g} \tag{6}$$

$$n_e \approx \frac{P}{V\alpha \mathrm{Ae}\left(\mu_0 E_0^{\omega}\right)E_x^{1-\omega}} \approx \frac{P}{V\alpha \mathrm{Ae}\left(\frac{V}{d}\frac{3\varepsilon_p}{2\varepsilon_p+\varepsilon_g}\right)^{1-\omega}} \tag{7}$$

$$E_e \approx \frac{P}{2 \times f \times V_r \times n_e \times 1.602 \times 10^{-25}} \tag{8}$$

where E_x is the average electrical field, n_e is the electron density, E_e is the mean electron energy, and V is the applied voltage. d denotes the separation distance between the electrodes; ε_g and ε_p denote the dielectric constants of background gas and packing pellets, respectively. In Eq. (7), α and A denotes the void fraction and cross-sectional area of packed bed reactor, respectively. In addition, e is the electric charge of electrons (equal to 1.6×10^{-19} C), μ_0 is the electron mobility at reference electric field, and V_r is reactor volume. E_0 and ω are empirical coefficients. Based on Eqs. (6), (7), and (8), we know that ε_p is linearly proportional to E_e. Thus, when the magnitude of ε_p is significantly high, the E_e would be enhanced. Carman and Mildren (2000) developed a model using an electron energy distribution function (EEDF) to quantify the plasma kinetics in dielectric barrier discharge. The result shows that the electron energy is directly related to the EEDF. On the other hand, EEDF greatly affects the coefficient of excitation (α_{ex}), coefficient of ionization (α_i), and electron transport (diffusion D_e and mobility μ_e).

Catalyst can provide the contact points on which numerous electrons can collide. The intense collision of electron may increase the discharge zone temperature. A study conducted by Yarahmadi and Alyar (2020) showed that the removal efficiency and the energy efficiency highly are highly dependent on the temperature of the discharge zone. Hence, the increase in the temperature of discharge zone could also increase of C_4F_8 conversion. The mean electron temperature can be calculated from swarm parameters of electrons in nitrogen as follows (Takaki et al. 2004):

$$kT_e/e \approx kT_{eo}(E/E_o)^{-\beta}/e \approx \mu_e/D_e \tag{9}$$

In Eq. (9), β denotes the power law constant, k denotes the Boltzmann constant (1.38×10^{-23} J/K), and D_e denotes the diffusion constant. Since an experimental value of μ_e/D_e is limited, the electron mean temperature can be determined from the plasma neutrality conditions ($n_e \fallingdotseq n_i$) after computing the total ion density (n_i). In our study, the energy efficiency and removal efficiency achieved with the plasma catalysis are 0.6–2 times higher than those achieved with NTP-alone system. Based on the analysis, the addition of a catalyst results in better performance of the plasma kinetic and plasma chemistry.

In plasma-based system, energetic electrons and active N_2 species are essential for C_4F_8 conversions. As previously mentioned, the C_4F_8 conversions increased with increasing applied voltage; as the applied voltage increases, the mean electric field and electron density should increase as well, resulting in the increase of C_4F_8 conversion achieved with plasma-based. Figure 6 indicates the energy efficiencies of non-thermal plasma and plasma catalysis system for C_4F_8 removal (for the same energy input). The removal rate of C_4F_8 achieved with non-thermal plasma is significantly lower than that obtained with the plasma catalysis system. The energy efficiencies achieved with non-thermal plasma and plasma catalysis are 0.25 g/kWh and 0.53 g/kWh, respectively. Here, the voltage of 12 kV is applied for both systems. As displayed in Fig. 6, the energy efficiency shows gradual decrease with increasing applied voltage. Basically, the increase of applied voltage might increase the power input. According to Eq. (2), increasing power input and conversion manifest different effects on energy efficiency. However, the downtrend of energy efficiency was expected with increasing power input, even though the C_4F_8 conversion might be increased. The results presented in Fig. 6 indicate that plasma catalysis could reach a higher energy efficiency in C_4F_8 conversion

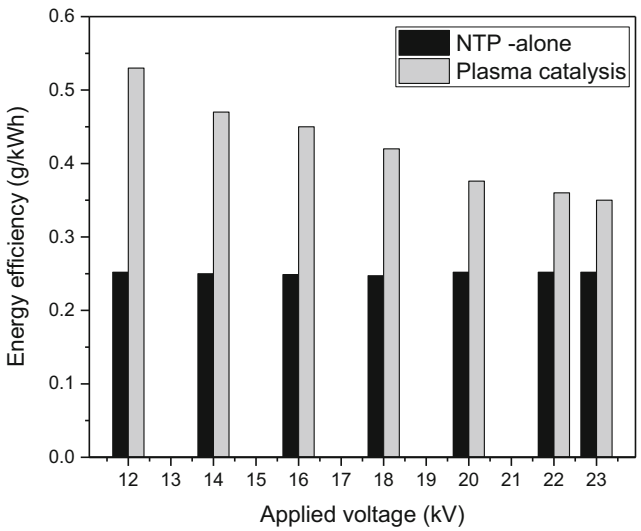

Fig. 6 Energy efficiencies of plasma-based systems for removing C_4F_8 achieved with non-thermal plasma and plasma catalysis, respectively, at various applied voltages ([C_4F_8] = 300 ppm, carrier gas = N_2, gas flow rate= 100 mL/min)

compared with non-thermal plasma at the same level of energy consumption. Applying density functional theory on the decomposition of c-C_4F_8 (cyclic-Octafluorocyclobutane), Xiao et al. (2018) reported that the reaction enthalpy required for c-C_4F_8 decomposition is 420 kJ/mol under trace water conditions. Zhang et al. (2018a, b) reported that the total reaction enthalpy required for c-C_4F_8 decomposition is 524 kcal/mol based on the ReaxFF MD simulation.

Effects of gas flow rate, inlet concentration, oxygen and argon contents on C_4F_8 removal

Figure 7 shows the effects of gas flow rate on C_4F_8 conversion obtained with plasma-based systems; gas flow rates of 100 mL/min, 500 mL/min, 1,000 mL/min, and 1,500 mL/min are imported individually into the plasma-based systems for C_4F_8 conversion. The plasma-based system is operated at applied voltage and frequency of 23 kV and 18.5 kHz, respectively, [C_4F_8] = 300 ppm and carrier gas = N_2. As shown in Fig. 7, as Q = 500 mL/min, the C_4F_8 conversion obtained with non-thermal plasma is 23.1% at applied voltage of 23 kV. Compared with Q = 100 mL/min, the C_4F_8 conversion obtained with non-thermal plasma is significantly lower. As the gas flow rate is further increased to 1500 mL/min (with the gas residence time of 1.1 second), the C_4F_8 conversion approaches 0%; the highest conversion is achieved at a flow rate 100 mL/min, corresponding to the gas residence time of 16.5 s. Overall, the highest energy efficiency with the plasma catalysis is 0.75 g/kWh at the gas flow rate of 500 mL/min, and conversion of 41 % is achieved with the gas residence time of 3.3 s. At the same power consumption, the conversion efficiency and gas flow rate are proportional to the energy efficiency. As shown in Fig. 7, increasing gas flow rate leads to decreasing residence time, resulting in lower C_4F_8 conversion. Figure 8 shows that the C_4F_8 conversion efficiency reaches

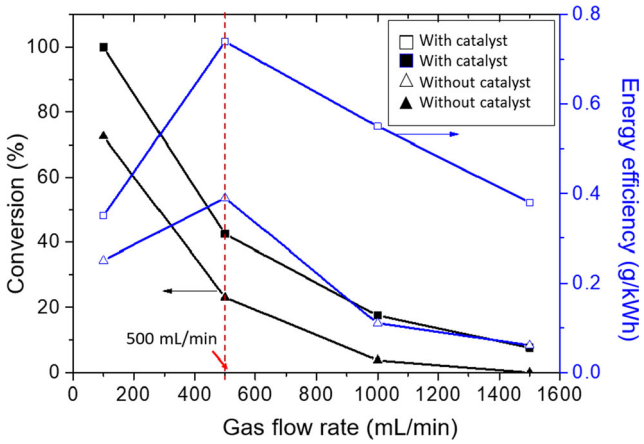

Fig. 7 Effects of gas flow rate on C_4F_8 conversion and energy efficiency ([C_4F_8] = 300 ppm, applied frequency= 18.5 kHz, applied voltage= 23 kV, and carrier gas = N_2)

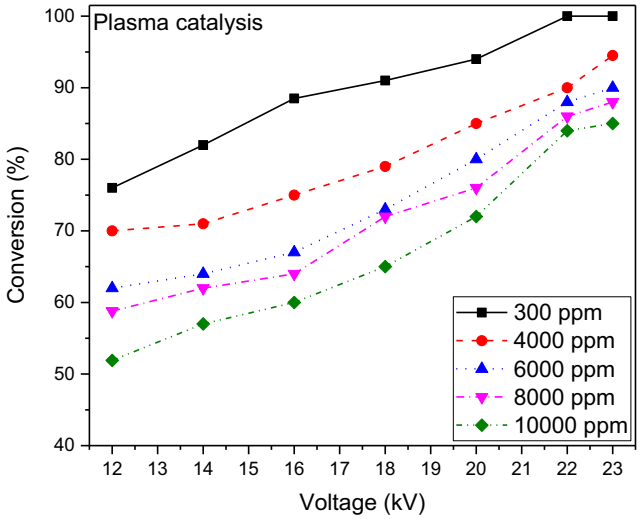

Fig. 8 Effects of C_4F_8 concentration on C_4F_8 conversion at various applied voltages (applied frequency= 18.5 kHz, gas flow rate = 100 mL/min, and carrier gas = N_2)

the highest value at a low concentration (300 ppm), and the conversion also increases with increasing applied voltage, i.e., from 36.8% at 12 kV to 72.6% at 23 kV. However, as C_4F_8 concentration increases, the C_4F_8 conversion efficiency decreases significantly. The C_4F_8 conversion efficiencies achieved are less than 20% for the inlet C_4F_8 concentrations ranging from 6000 to 10,000 ppm. The overall trend of the plasma catalysis system is similar to that of the non-thermal plasma system, except that higher conversion efficiency is obtained. Figure 9 shows the performance of plasma catalysis evaluated with the addition of O_2 content varying from 0 to 5% O_2. The purpose of adding oxygen to the gas stream is to increase the generation of active species which are beneficial to C_4F_8 oxidation. In fact, if oxygen is absent, lattice oxygen

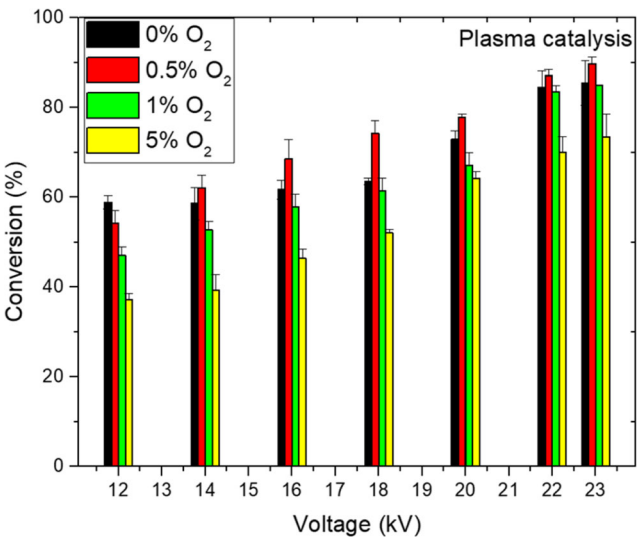

Fig. 9 Effects of oxygen content on the performance of plasma catalysis for C_4F_8 removal ([C_4F_8] = 10,000 ppm, applied frequency= 18.5 kHz, gas flow rate = 100 mL/min, and carrier gas = N_2)

from Al_2O_3 and O species from etching quartz (SiO_2) could help oxidize C_4F_8. However, the results show that the addition of 0.5% oxygen can increase C_4F_8 conversion and then decrease if too much O_2 is added. These phenomena could explain that O_2 molecules themselves will turn into active species such O^+, O^-, O_2^+, and O_2^-. These active species will react with C_4F_8 to form CO_2, CO, and COF_2. However, too much oxygen in the plasma system may reduce C_4F_8 conversion because O_2 is an electronegative gas to which electrons would attach. As a consequence, the electron density may be reduced, resulting in lower C_4F_8 conversion. Similar trends were observed in the decomposition of fluorinated compounds with non-thermal plasma as reported by Gandhi and Mok (2012) and Wallis et al. (2007). The best C_4F_8 conversion reached 89% with the O_2 content of 0.5% at applied voltage of 23 kV. Furthermore, addition of oxygen into N_2-C_XF_Y gas mixture may form several products such as CO, CO_2, COF_2, OF_2, NO, NO_2, N_2O, FO, FO_2, FNO, FNO_2, and $FONO_2$. Downward trend of C_4F_8 conversion with increasing O_2 is partly attributed to the reactions of O_2 with some N_2^* and $N_2(A^3\sum_u^+)$ to form NO_x, resulting in lower C_4F_8 conversion. Kim et al. (2008) and Xie et al. (2009) indicate that energetic electrons react with excess oxygen; the collision might occur to form other compounds, which in turn, decrease the PFCs decomposition efficiency. O_3 formation might occur in the non-thermal plasma system when O_2 is added into the system. Since the reaction rate constant is relatively low as reported by Vasenkov et al. (2004), the presence of O_3 has a minor effect on C_4F_8 removal; the mechanism regarding C_4F_8 removal via the reactions with O^+, O^-, O_2^+, O_2^-, and O_3. could be described in reactions (10)–(18):

Reaction	Rate constant ($cm^3\ s^{-1}$)	
$O^+ + C_4F_8 \rightarrow C_4F_8^+ + O$	1.22×10^{-9}	(10)
$O_2^+ + C_4F_8 \rightarrow C_4F_8^+ + O_2$	1.55×10^{-9}	(11)
$O^+ + C_4F_8 \rightarrow C_3F_5^+ + CF_3^+ + O$	0.76×10^{-9}	(12)
$O^+ + C_4F_8 \rightarrow C_4F_7^+ + F^+ + O$	0.28×10^{-9}	(13)
$O_2^+ + C_4F_8 \rightarrow C_2F_4^+ + C_2F_4 + O_2$	4.48×10^{-10}	(14)
$O_2^+ + C_4F_8 \rightarrow C_3F_5^+ + CF_3 + O_2$	1.15×10^{-9}	(15)
$O_2^- + C_4F_8 \rightarrow C_4F_8^- + O_2$	4.60×10^{-10}	(16)
$O^- + C_4F_8 \rightarrow C_4F_8^- + O$	1.0×10^{-10}	(17)
$O_3 + C_4F_8 \rightarrow$ Adduct	1.83×10^{-18}	(18)

To evaluate the effect of Ar addition on C_4F_8 conversion, various Ar contents ranging from 1 to 20% are introduced into the system. In general, formation of active species in plasma is a very complicated process; it consists of electrons, ions, and exciting species. Ar is considered as a good carrier gas in the plasma process because it can easily be excited to metastable state (Ar*). Compared with N_2, Ar* has several advantages such as a high threshold energy of 13 eV and lower dielectric strength. The effect of Ar contents on the performance of plasma catalysis for C_4F_8 removals with the presence of 5% O_2 is shown in Fig. 10, indicating that the adverse effects caused by O_2 on C_4F_8 removal is mitigated with increasing Ar content. Specifically, C_4F_8 conversions obtained with plasma catalysis reaches 100% as Ar content is controlled at 20%, with the applied voltage of 22 and 23 kV even in the presence of 5% O_2. According to Vasenkov et al. (2004), the mechanism regarding C_4F_8 removal via the reactions with Ar^+ or Ar* could be described in reactions (19)–(23):

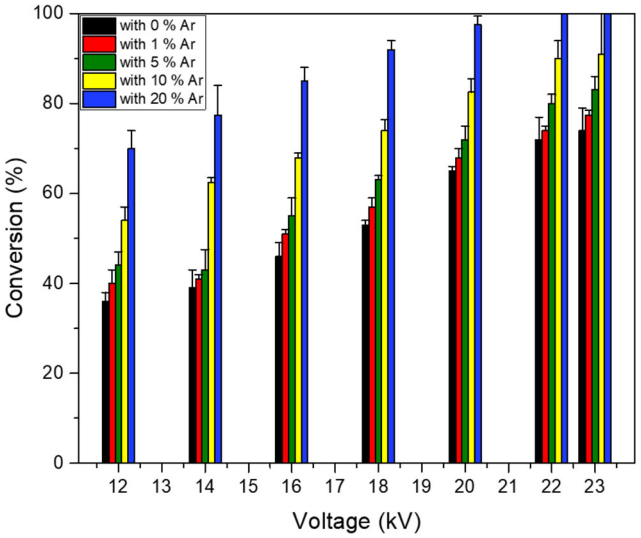

Fig. 10 Effect of Ar contents on the performance of plasma catalysis in the presence of 5% O_2, ([C_4F_8] = 10,000 ppm, gas flow rate =100 mL/min, applied frequency 18.5 kHz, and carrier gas = N_2)

$$e + Ar \rightarrow Ar^+ \text{ or } Ar^* \quad (19)$$

$$Ar^+ + C_4F_8 \rightarrow CF_3^+ + C_3F_5 + Ar \quad (20)$$

$$Ar^+ + C_4F_8 \rightarrow C_3F_5^+ + CF_3 + Ar \quad (21)$$

$$Ar^* + C_4F_8 \rightarrow C_2F_4^+ + C_2F_4 + Ar \quad (22)$$

$$Ar^* + C_4F_8 \rightarrow CF^+ + C_3F_7 + Ar \quad (23)$$

Conclusion

In this study, decomposition of C_4F_8 was investigated with three systems, i.e., catalytic hydrolysis, non-thermal plasma, and plasma catalysis. Decomposition of C_4F_8 obtained with catalytic hydrolysis reaches the highest efficiency of 20.1%, being obtained with γ-Al_2O_3 as catalyst in the presence of 10% $H_2O_{(g)}$ and operating temperature of 800 °C. A non-thermal plasma system was established to investigate the efficiency of converting C_4F_8. As N_2 is applied as carrier gas in

the non-thermal plasma system, the conversion efficiencies of C_4F_8 are up to 72%. Regarding the influence of the gas flow rate, as the non-thermal plasma system is operated at 500 mL/min, the C_4F_8 conversion decreases significantly, indicating that appropriate gas residence time is needed for non-thermal plasma system towards effective removal of C_4F_8. As the system is operated at 22 kV, C_4F_8 conversion also reaches 100% achieved via plasma catalysis. The effect of O_2 content on plasma catalysis shows that the conversion of C_4F_8 decreases as 1 to 5% O_2 is added into the system. This is due to the reaction of O_2 with N_2^* and $N_2(A^3\sum_u^+)$; furthermore, O_2 gas has electronegative property due to the electron attachment to the oxygen molecules, resulting in lower C_4F_8 conversion. As the O_2 content is reduced to 0.5%, the results show that C_4F_8 conversions increase. It is because other species formed in the plasma reaction combine with O_2 to inhibit recombinations of C_4F_8. In terms of the influence of Ar content, the results show that the conversion efficiency of C_4F_8 increases significantly with increasing Ar content, indicating that the addition of appropriate Ar content into the plasma system poses a positive effect on C_4F_8 removal.

Supplementary Information The online version contains supplementary material available at https://doi.org/10.1007/s11356-021-14649-0.

Availability of data and materials All data generated or analyzed during this study are included in this published article [and its supplementary information files].

Authors' contributions Ya Sheng developed and designed the methodology of this experiment and prepared the original draft. Kuan Lun reviewed and edit the published work by those from the original research group. Moo Been Chang supervised the project and had the oversight and leadership responsibility for the research activity planning and execution, including mentorship external to the core team. All authors read and approved the final manuscript."

Funding This study was financially supported by TSMC (Taiwan Semiconductor Manufacturing Company).

Declarations

Ethics approval and consent to participate Not applicable

Consent for publication Not applicable

Consent to Publish Not applicable

Competing interests Not applicable

References

Carman RJ, Mildren RP (2000) Electron energy distribution functions for modeling the plasma kineticts in dielectrical barrier discharges. J Phys D: Appl 33:L99–L103. https://doi.org/10.1088/0022-3727/33/19/101/meta

Chang MB, Chang JS (2006) Abatement of PFCs from semiconductor manufacturing processes by nonthermal plasma technologies. A critical review. Ind Eng Chem Res 45:4101–4109. https://doi.org/10.1021/ie051227b

Chang MB, Lee HM (2004) Abatement of perfluorocarbons with combined plasma catalysis in atmospheric-pressure environment. Catal Today 89:109–115. https://doi.org/10.1016/j.cattod.2003.11.016

Chang MB, Yu SJ (2001) An atmospheric-pressure plasma process for C_2F_6 removal. Environt Sci Techno 35:1587–1592. https://doi.org/10.1021/es001556p

Chen HL, Lee HM, Chen SH, Chao Y, Chang MB (2008) Review of plasma catalysis on hydrocarbon reforming for hydrogen production—interaction, integration, and prospects. Appl Catal B Environ 85:1–9. https://doi.org/10.1016/j.apcatb.2008.06.021

Chen JX, Pan KL, Yu SJ, Yen SJ, Chang MB (2017) Combined fast selective reduction using Mn-based catalysts and nonthermal plasma for NO_x removal. Environ Sci Pollut Res 24:21496–21508. https://doi.org/10.1007/s11356-017-9785-8

Choi S, Hong SH, Lee HS, Watanabe A (2012) A comparative study of air and nitrogen thermal plasmas for PFCs decomposition. Chem Eng J 185:193–200. https://doi.org/10.1016/j.cej.2012.01.077

El-Bahy Z, Ohnishi R, Ichikawa M (2003) Hydrolysis of CF_4 over alumina-based binary metal oxide catalysts. Appl Catal B Environ 40:81–91. https://doi.org/10.1016/S0926-3373(02)00143-1

Futamura S, Gurusamy A (2005) Synergy of nonthermal plasma and catalysts in the decomposition of fluorinated hydrocarbons. J Electrost 63:949–954. https://doi.org/10.1016/j.elstat.2005.03.067

Futamura S, Einaga H, Zhang A (2001) Comparison of reactor performance in the nonthermal plasma chemical processing of hazardous air pollutants. IEEE Trans Ind Appl 37:978–985. https://doi.org/10.1109/28.936387

Gandhi MS, Mok YS (2012) Decomposition of trifluoromethane in a dielectric barrier discharge non-thermal plasma reactor. J Environ Sci 24:1234–1239 S1001074211609352

Gao SH, GaoLH ZKS (2011) Super-hydrophobicity and oleophobicity of silicone rubber modified by CF_4 radio frequency plasma. Appl Surf Sci 257:4945–4950. https://doi.org/10.1016/j.apsusc.2011.01.001

Hannus I (1999) Adsorption and transformation of halogenated hydrocarbons over zeolites. Appl Cataly A Gen 189:263–276. https://doi.org/10.1016/S0926-860X(99)00283-5

Hayashi N, Satoh S (2005) Treatment of a perfluorocarbon using nonthermal plasma produced by atmospheric streamer corona discharge. IEEE Trans Plasma Sci 33:274–275. https://doi.org/10.1109/TPS.2005.845003

Jia L, Ma S (2005) The experimental study on high temperature air combustion and CF_4 decomposition. Heat Transf Summer Conf 1:705–708. https://doi.org/10.1115/HT2005-72440

Jia W, Jin L, Wang Y, Lu J, Luo M (2011) Fluorination of dichlorodifluoromethane to synthesize tetrafluoromethane over Cr_2O_3–AlF_3 catalyst. J Ind Eng Chem 17:615–620. https://doi.org/10.1016/j.jiec.2011.05.005

Jie FAN, Xiu-Feng XU, Xian-Jun NIU (2008) Decomposition of CF_4 over Al_2O_3-based metal oxides. Acta Physico-Chimica Sin 24:1271–1276. https://doi.org/10.3866/pku.whxb20080725

Kim HH, Ogata A, Futamura S (2008) Oxygen partial pressure-dependent behavior of various catalysts for the total oxidation of VOCs using cycled system of adsorption and oxygen plasma. Appl Catal B Environ 79:356–367. https://doi.org/10.1016/j.apcatb.2007.10.038

Kuroki T, Mine J, Odahara S, Okubo M, Yamamoto T, Saeki N (2005) CF_4 decomposition of flue gas from semiconductor process using inductively coupled plasma. IEEE Trans Ind Appl 41:221–228. https://doi.org/10.1109/TIA.2004.840954

Lee HM, Chen SH (2017) Thermal abatement of perfluorocompounds with plasma torches. Energy Procedia 142:3637–3643. https://doi.org/10.1016/j.egypro.2017.12.256

Lee YC, Jeon JK (2012) A study on catalytic process in pilot plant for abatement of PFC emission. Clean Technol 18:216–220. https://doi.org/10.7464/ksct.2012.18.2.216

Lin BY, Chang MB, Chen HL, Lee HM, Yu SJ, Li SN (2011) Removal of C_3F_8 via the combination of non-thermal plasma, adsorption and catalysis. Plasma Chem Plasma Process 31:585–594. https://doi.org/10.1007/s11090-011-9303-6

Pan KL, Chen YS, Chang MB (2019) Effective removal of CF_4 by combining nonthermal plasma with γ-Al_2O_3. Plasma Chem Plasma Process 39:877–896. https://doi.org/10.1007/s11090-019-09990-9

Park NK, Park HG, Lee TJ, Chang WC, Kwon WT (2012) Hydrolysis and oxidation on supported phosphate catalyst for decomposition of SF_6. Catal Today 185:247–252. https://doi.org/10.1016/j.cattod.2011.08.008

Radoiu MT (2004) Studies on atmospheric plasma abatement of PFCs. Radiat Phys Chem 69:113–120. https://doi.org/10.1016/S0969-806X(03)00455-9

Song JY, Chung SH, Kim MS, Seo MG, Lee YH, Lee KY, Kim JS (2013) The catalytic decomposition of CF_4 over Ce/Al_2O_3 modified by a cerium sulfate precursor. J Mol Catal A Chem 370:50–55. https://doi.org/10.1016/j.molcata.2012.12.011

Suzuki K, Ishihira Y, Sakoda K, Shirai Y, Teramoto A, Hirayama M, Ohmi T, Watanabe T, Ito T (2008) High-efficiency PFC abatement system utilizing plasma decomposition and Ca(OH)2/CaO immobilization. IEEE Trans Semiconductor Manuf 21:668–675. https://doi.org/10.1109/TSM.2008.2005400

Takaki K, Chang JS, Kostov KG (2004) Atmospheric pressure of nitrogen plasmas in a ferro-electric packed bed barrier discharge reactor part I: modeling. IEEE Trans Dielect Elect Insul 11:481–490. https://doi.org/10.1109/TDEI.2004.1306726

Takita Y, Ninomiya M, Miyake H, Wakamatsu H, Yoshinaga Y, Ishihara T (1999) Catalytic decomposition of perfluorocarbons Part II. Decomposition of CF_4 over $AlPO_4$-rare earth phosphate catalysts. Phys Chem Chem Phys 1:4501–4504. https://doi.org/10.1039/a904311j

Takita Y, Tanabe T, Ito M, Ogura M, Muraya T, Yasuda S, Nishiguchi H, Ishihara T (2002) Decomposition of CH_2FCF_3 (134a) over metal phosphate catalysts. Ind Eng Chem Res 41:2585–2590. https://doi.org/10.1021/ie0106229

Vasenkov AV, Li X, Oehrlein GS, Kushner MJ (2004) Properties of c-C_4F_8 inductively coupled plasmas. II. Plasma chemistry and reaction mechanism for modeling of Ar/c-C_4F_8/O_2 discharges. J Vac Sci Technol A Vacuum, Surfaces ,Films 22:511–530. https://doi.org/10.1116/1.1697483

Wallis AE, Whitehead JC, Zhang K (2007) Plasma-assisted catalysis for the destruction of CFC-12 in atmospheric pressure gas streams using TiO_2. Catatysis Lett 113:29–33. https://doi.org/10.1007/s10562-006-9000-x

Xiao S, Li Y, Zhang X, Zhuo R, Wang D, Tang J, Zhang J, Chen Q (2018) Influence of trace water on decomposition mechanism of c-C_4F_8 as environmental friendly insulating gas at high temperature. AIP Adv 8:125202. https://doi.org/10.1063/1.5044751

Xie HD, Sun B, Zhu XM, Liu YJ (2009) Influence of O_2 on the CF_4 decomposition by atmospheric microwave plasma. Int J Plasma Environ Sci Technol 3:39–42. https://doi.org/10.1088/0022-3727/47/35/355205

Yarahmadi R, Alyar S (2020) A Laboratory study of low-temperature co removal from mobile exhaust gas using in-plasma catalysis. Emiss Control Sci Technol 6:17–27. https://doi.org/10.1007/s40825-020-00154-2

Zhang X, Xiao H, Hu X, Gui Y (2016) Effects of background gas on sulfur hexafluoride removal by atmospheric dielectric barrier discharge plasma. AIP Adv 6:115005. https://doi.org/10.1063/1.4967277

Zhang X, Zhang G, Wu Y, Song S (2018a) Synergistic treatment of SF_6 by dielectric barrier discharge/γ-Al_2O_3 catalysis. AIP Adv 8:125109. https://doi.org/10.1063/1.5054729

Zhang Y, Li Y, Zhang X, Xiao S, Tang J (2018b) Insights on decomposition process of c-C_4F_8 and c-C_4F_8/N_2 mixture as substitutes for SF_6. R Soc Open Sci 5:81104. https://doi.org/10.1098/rsos.181104